

# Investigation on the microstructure and electrochemical performances of as-cast and quenched $\text{La}_{0.7}\text{Mg}_{0.3}\text{Co}_{0.45}\text{Ni}_{2.55-x}\text{M}_x$ ( $\text{M} = \text{Cu}, \text{Al}, \text{Mn}; x = 0-0.4$ ) electrode alloys

Yang-huan Zhang<sup>a,b,\*</sup>, Dong-liang Zhao<sup>a</sup>, Hui-ping Ren<sup>b</sup>,  
Zhong-wang Wu<sup>b</sup>, Xiao-ping Dong<sup>a,c</sup>, Xin-lin Wang<sup>a</sup>

<sup>a</sup> Department of Functional Material Research, Central Iron and Steel Research Institute, Beijing, China

<sup>b</sup> School of Material, Inner Mongolia University of Science and Technology, Baotou, China

<sup>c</sup> School of Material Science and Engineering, University of Science and Technology, Beijing 100083, China

Received 14 September 2006; received in revised form 10 January 2007; accepted 19 February 2007

Available online 25 February 2007

## Abstract

A new La–Mg–Ni system (PuNi<sub>3</sub>-type)  $\text{La}_{0.7}\text{Mg}_{0.3}\text{Co}_{0.45}\text{Ni}_{2.55-x}\text{M}_x$  ( $\text{M} = \text{Cu}, \text{Al}, \text{Mn}; x = 0, 0.1, 0.2, 0.3, 0.4$ ) electrode alloys were prepared by casting and rapid quenching. The effects of element substitution and rapid quenching on the microstructures and electrochemical performances of the alloys were investigated. The results obtained by XRD, SEM and TEM show that the alloys have a multiphase structure, including the (La, Mg)Ni<sub>3</sub>, the LaNi<sub>5</sub> and the LaNi<sub>2</sub> phases. The substitution of Cu for Ni promotes the formation of an amorphous phase in the as-quenched alloy, and a reversal result produced by the substitution of Al for Ni. The electrochemical measurement indicates that the element substitution decreases the discharge capacity of the alloys, whereas it obviously improved the cycle stability of the alloys. The positive influence of three kinds of substitution elements on the cycle life of the alloys is in the sequence Al > Cu > Mn, and the negative influence on the discharge capacity in the sequence Al > Mn > Cu.

© 2007 Published by Elsevier B.V.

**Keywords:** Element substitution; La–Mg–Ni system electrode alloy; Rapid quenching; Microstructures; Electrochemical performances

## 1. Introduction

Since the commercialization of small size Ni–MH cells in 1990, the small size Ni–MH cells have rapidly grown and gained a good share in the rechargeable battery market. In the very recent years, however, the rechargeable Ni–MH cells are encountering serious competition owing to rapid development of Li-ion cells. Therefore, the investigation of new type electrode alloy with higher discharge capacity and longer cycle life is very important to exalt the competition ability of Ni–MH batteries in

the rechargeable battery field. Several new and good hydrogen storage alloys were reported recently [1–3]. The most promising candidates are the La–Mg–Ni based alloys in view of their higher electrochemical capacities (360–410 mAh/g) and low production costs. However, for commercial application, the rather poor cycle stability of the La–Mg–Ni based alloys has to be further improved. As is known to all, element substitution is one of the effective methods for improving the overall properties of the hydrogen storage alloys [4,5], and the preparation technology also is extremely important for improving the performances of the alloys. Therefore, it is expected that an optimized amount of substituting Ni with M ( $\text{M} = \text{Cu}, \text{Al}$  and  $\text{Mn}$ ) in La–Mg–Ni system alloy and a selected rapid quenching technique may produce an alloy with high discharge capacity and good cycling stability. Therefore, the effects of the element substitution on the microstructures and the electrochemical properties of the

\* Corresponding author at: Department of Functional Material Research, Central Iron and Steel Research Institute, 76 Xueyuan Nan Road, Haidian District, 100081 Beijing, China. Tel.: +86 10 62187570; fax: +86 10 62182296.

E-mail addresses: zyh59@yahoo.com.cn,  
wangxinlin@vip.163.com (Y.-h. Zhang).

$\text{La}_{0.7}\text{Mg}_{0.3}\text{Ni}_{2.55-x}\text{Co}_{0.45}\text{M}_x$  ( $M = \text{Cu}, \text{Al}, \text{Mn}; x = 0-0.4$ ) electrode alloys were systematically investigated.

## 2. Experimental

The nominal composition of the alloys is  $\text{La}_{0.7}\text{Mg}_{0.3}\text{Co}_{0.45}\text{Ni}_{2.55-x}\text{M}_x$  ( $M = \text{Cu}, \text{Al}, \text{Mn}; x = 0, 0.1, 0.2, 0.3, 0.4$ ), and corresponding with  $M$  content  $x$ , the alloys are represented by  $M_0, M_1, M_2, M_3$  and  $M_4$ , respectively. The alloys were melted in an argon atmosphere using a vacuum induction furnace. The purity of all the component metals is at least 99.8%. Part of the as-cast alloys was quenched by melt-spinning with a rotating copper wheel. The quenching rate is expressed by the linear velocity of the copper wheel and the quenching rates used in the experiment are 15, 20, 25 and 30 m/s.

The phase structures and composition of the alloys were determined by XRD diffractometer of D/max/2400. The diffraction was performed with  $\text{Cu K}\alpha 1$  radiation filtered by graphite. The experimental parameters for determining phase structure are 160 mA, 40 kV and  $10^\circ/\text{min}$ , respectively. The morphologies and the crystalline states of the as-quenched alloys were determined by TEM.

A round electrode pellet 15 mm in diameter was prepared by mixing 1 g of alloy powder with fine nickel powder in a weight ratio of 1:1 together with a small amount of polyvinyl alcohol (PVA) solution as binder, and then compressed under a pressure of 35 MPa. The experimental electrodes were tested in a tri-electrode open cell, consisting of a metal hydride working electrode, a  $\text{NiOOH}/\text{Ni}(\text{OH})_2$  counter electrode and a  $\text{Hg}/\text{HgO}$  reference electrode. The electrolyte was a 6 M KOH solution. The voltage between the negative electrode and the reference electrode is defined as the discharge voltage. Every cycle was charged with a constant current of 100 mA/g for 5 h, resting 15 min and then discharged at 100 mA/g to a  $-0.500$  V cut-off voltage. The environment temperature of the measurement was kept at  $30^\circ\text{C}$ .

## 3. Results and discussion

### 3.1. Microstructure

The phase composition and structure of the as-cast and quenched alloys analysed by XRD were shown in Fig. 1. The alloys have a multiphase structure, composing of the  $(\text{La}, \text{Mg})\text{Ni}_3$ , the  $\text{LaNi}_5$  and the  $\text{LaNi}_2$  phases. The substitution of Cu, Al and Mn for Ni and rapid quenching have an inappreciable influence on the phase compositions of the alloys, but both changed the phase abundances of the alloys. For the as-cast alloys, the element substitution produced an increasing tendency of the  $\text{LaNi}_2$  phase, and substituting Ni with Al or Mn is especially obvious. The lattice parameters of the  $\text{LaNi}_5$  and  $(\text{La}, \text{Mg})\text{Ni}_3$  main phases in the as-cast and quenched ( $20 \text{ m/s}$ )  $M_2$  ( $M = \text{Cu}, \text{Al}$  and  $\text{Mn}$ ) alloys, which were calculated from the XRD data by a method of least squares, were listed in Table 1. The results in Table 1 indicate that the rapid quenching leads

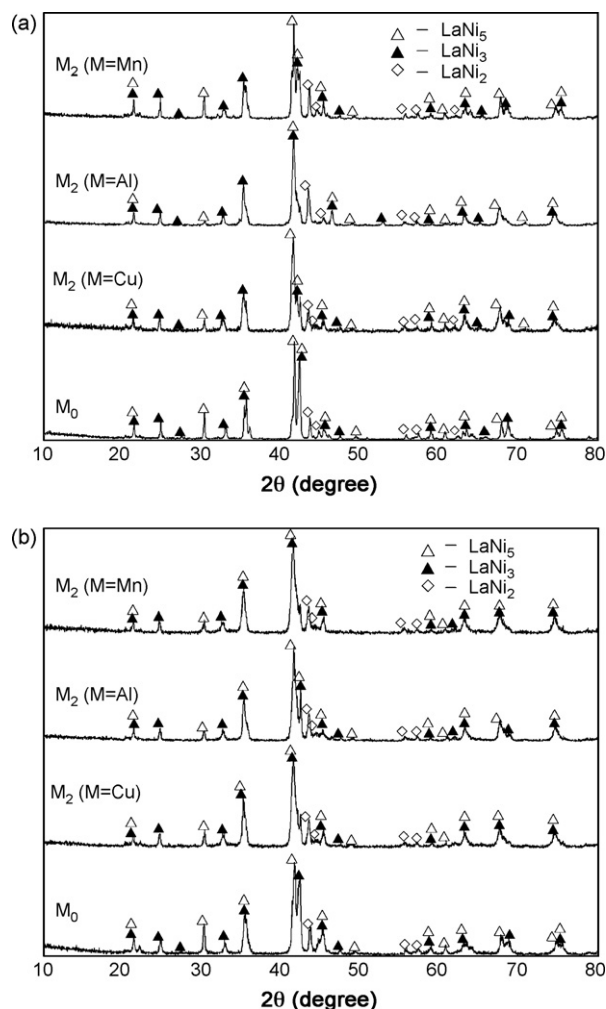


Fig. 1. The X-ray diffraction patterns of the: (a) as-cast and (b) as-quenched ( $20 \text{ m/s}$ ) alloys.

to an increase of  $c$  axis and a slight decrease of  $a$  axis and cell volumes of the  $\text{LaNi}_5$  and  $(\text{La}, \text{Mg})\text{Ni}_3$  main phases. The element substitution obviously increases the lattice parameters and cell volumes of the  $\text{LaNi}_5$  and  $(\text{La}, \text{Mg})\text{Ni}_3$  main phases in the as-cast and quenched alloys, for which Cu, Al and Mn atoms occupy the lattice sites of Ni atoms is responsible since their atom radius are larger than that of Ni.

The morphologies and the crystalline state of the as-quenched alloys examined by TEM are shown in Fig. 2. The results in

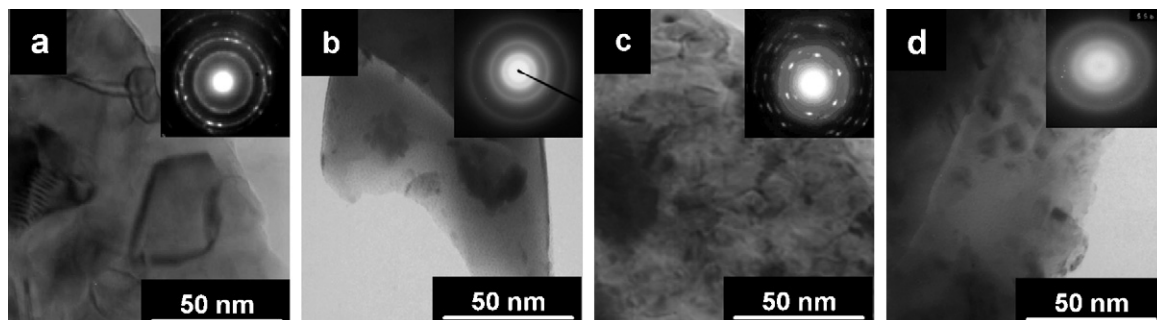


Fig. 2. The morphologies and SAD of the as-quenched ( $20 \text{ m/s}$ ) alloys taken by TEM: (a)  $M_0$  alloy; (b–d)  $M_2$  ( $M = \text{Cu}, \text{Al}$  and  $\text{Mn}$ ) alloys.

Table 1  
Lattice parameters and cell volume of the LaNi<sub>5</sub> and (La, Mg)Ni<sub>3</sub> main phases

Conditions	Alloys	Main phases	Lattice constants (nm)		Cell volume (nm <sup>3</sup> )
			<i>a</i>	<i>c</i>	
As-cast	M <sub>0</sub>	(La, Mg)Ni <sub>3</sub>	0.5053	2.4317	0.5377
		LaNi <sub>5</sub>	0.5031	0.4043	0.0886
	M <sub>2</sub> (M = Cu)	(La, Mg)Ni <sub>3</sub>	0.506	2.4324	0.5393
		LaNi <sub>5</sub>	0.5036	0.4051	0.0889
	M <sub>4</sub> (M = Cu)	(La, Mg)Ni <sub>3</sub>	0.5063	2.4338	0.5403
		LaNi <sub>5</sub>	0.5039	0.4057	0.0892
	M <sub>2</sub> (M = Al)	(La, Mg)Ni <sub>3</sub>	0.5062	2.4642	0.5468
		LaNi <sub>5</sub>	0.5038	0.4053	0.0891
	M <sub>4</sub> (M = Al)	(La, Mg)Ni <sub>3</sub>	0.5071	2.4703	0.5501
		LaNi <sub>5</sub>	0.5049	0.4063	0.0897
	M <sub>2</sub> (M = Mn)	(La, Mg)Ni <sub>3</sub>	0.5061	2.4405	0.5413
		LaNi <sub>5</sub>	0.5036	0.4053	0.089
M <sub>4</sub> (M = Mn)	(La, Mg)Ni <sub>3</sub>	0.5066	2.4464	0.5437	
	LaNi <sub>5</sub>	0.5041	0.4059	0.0893	
As-quenched (20 m/s)	M <sub>0</sub>	(La, Mg)Ni <sub>3</sub>	0.5046	2.4334	0.5366
		LaNi <sub>5</sub>	0.5025	0.4052	0.0886
	M <sub>2</sub> (M = Cu)	(La, Mg)Ni <sub>3</sub>	0.5055	2.4341	0.5386
		LaNi <sub>5</sub>	0.5031	0.4057	0.0889
	M <sub>4</sub> (M = Cu)	(La, Mg)Ni <sub>3</sub>	0.506	2.4352	0.5394
		LaNi <sub>5</sub>	0.5034	0.4064	0.0892
	M <sub>2</sub> (M = Al)	(La, Mg)Ni <sub>3</sub>	0.5054	2.4662	0.5455
		LaNi <sub>5</sub>	0.5031	0.4062	0.089
	M <sub>4</sub> (M = Al)	(La, Mg)Ni <sub>3</sub>	0.5063	2.4712	0.5486
		LaNi <sub>5</sub>	0.5042	0.4071	0.0896
	M <sub>2</sub> (M = Mn)	(La, Mg)Ni <sub>3</sub>	0.5049	2.4512	0.5411
		LaNi <sub>5</sub>	0.5031	0.4058	0.0889
M <sub>4</sub> (M = Mn)	(La, Mg)Ni <sub>3</sub>	0.5061	2.4469	0.5428	
	LaNi <sub>5</sub>	0.5038	0.4066	0.0893	

Fig. 2 indicate that as-quenched (20 m/s) M<sub>2</sub> (M = Cu and Mn) alloys have a tendency of the formation of an amorphous phase, whereas the as-quenched (20 m/s) M<sub>0</sub> and M<sub>2</sub> (M = Al) alloys have a typical micro-crystal and nano-crystal structure, implying that the substitution of Cu and Mn for Ni is favourable to the formation of an amorphous phase, but the substitution of Al for Ni is unfavourable. It needs to be noticed that the XRD patterns of the as-quenched Cu- and Mn-substituted alloys suggest their high crystalline, which is probably ascribed to the amount of amorphous phase in the as-quenched alloys is very small.

### 3.2. Electrochemical characteristics

#### 3.2.1. Discharge capacity

The M (M = Cu, Cr, Mn) content dependence of the maximum discharge capacity of the as-quenched (20 m/s) alloys was illustrated in Fig. 3. It can be derived from Fig. 3 that the capacities of the alloys decreased with increasing M content. When M content increased from 0 to 0.4, the capacity of M<sub>x</sub> (M = Cu) alloy decreased from 386.4 to 369.3 mAh/g, for M<sub>x</sub> (M = Al) alloy from 386.4 to 317.8 mAh/g, and for M<sub>x</sub> (M = Mn) alloy from

386.4 to 361.18 mAh/g. The negative effect of three kinds of substitution elements on the capacity of the alloys is in the sequence Cu < Mn < Al. The quenching rate dependence of the discharge capacities of the M<sub>0</sub> and M<sub>2</sub> (M = Cu, Al and Mn) alloys was

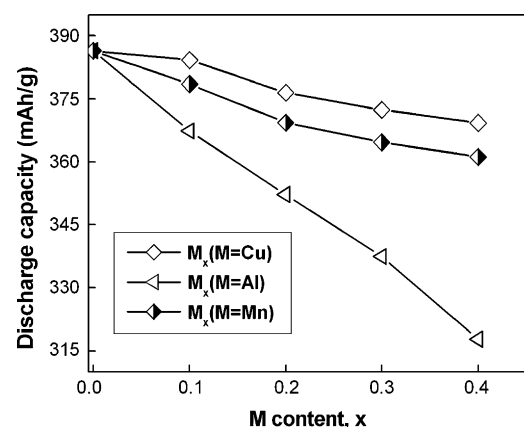


Fig. 3. The M content dependence of the discharge capacity of the as-quenched (20 m/s) alloys.

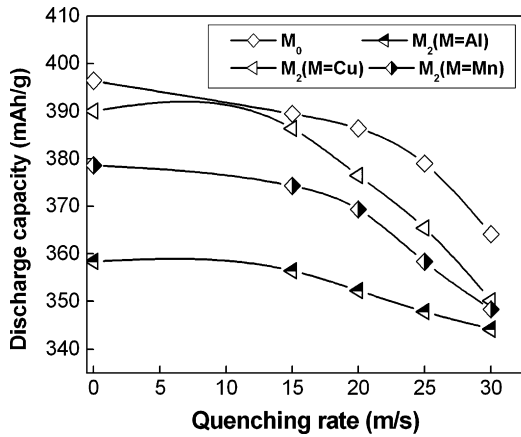


Fig. 4. The quenching rate dependence of the discharge capacity of  $M_0$  and  $M_2$  alloys.

shown in Fig. 4. Fig. 4 shows that the capacities of the alloys reduced with the incremental change of the quenching rate, but the decreased extent of the capacity of  $M_0$  and  $M_2$  ( $M=Cu$  and  $Mn$ ) is obviously larger than that of the  $M_2$  ( $M=Al$ ). When the quenching rate enhanced from 0 m/s (As-cast was defined as quenching rate of 0 m/s) to 30 m/s, the capacity of  $M_0$  and  $M_2$  ( $M=Cu$  and  $Mn$ ) alloys decreased from 396.4, 390.1 and 378.63 mAh/g to 364.1, 350.2 and 348.31 mAh/g, respectively, and for  $M_2$  ( $M=Al$ ) alloy from 358.4 to 344.2 mAh/g.

### 3.2.2. Discharge voltage characteristic

The discharge voltage curves of the as-cast and quenched alloys were shown in Fig. 5. The figure shows that the substitution of Cu for Ni enhanced slightly the discharge voltage, but obviously decreased the discharge voltage of the as-quenched alloy. The influence of Mn substitution on the discharge voltage of the as-cast alloy is inappreciable, but the substitution of Al significantly decreases the discharge voltages of the as-cast and quenched alloys. Especially, substituting Ni with Al not only decreased the discharge potential but also increased the slopes of the discharge potential plateaus of the as-cast and quenched alloys. Generally, the plateau voltage is closely relative to internal resistance of the battery, including ohmic internal resistance and polarization resistance. The discharge reaction of the hydrogen storage electrode mainly depends on the diffusion of hydrogen atoms in the alloy, and internal resistance of the alloy electrode reduces with the increase of the diffusion coefficient of the hydrogen atom [6]. The substitution of Cu, Mn and Al for Ni leads to a sharp reduction of the diffusion coefficient of the hydrogen atom, and the order of the diffusion coefficient is in sequence  $Al < Mn < Cu$ , for which an oxidation layer on the surface of the alloy electrode is mainly responsible. But Mn substituted alloy electrode, due to the oxidation of Mn dissolve subsequently in an alkaline electrolytic solution, can generate a porous surface, which conduces a slight melioration of the discharge reaction of the alloy electrode [7].

### 3.2.3. Cycle life

The cycle life, indicated by  $N$ , is characterized by the cycle number after which the discharge capacity of the alloy at a cur-

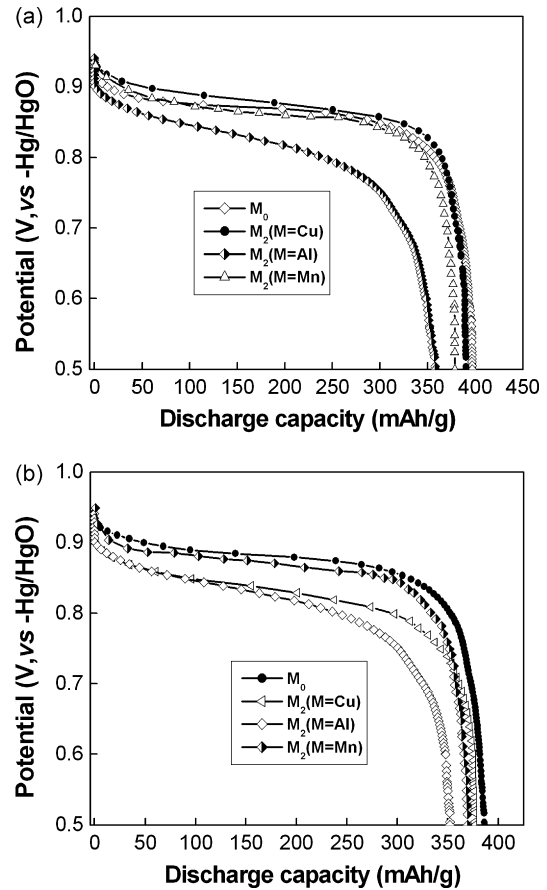


Fig. 5. The discharge potential curves of the: (a) as-cast and (b) as-quenched (20 m/s) alloys.

rent density of 100 mA/g is reduced to 60% of the maximum capacity. The M content dependence of the cycle lives of the alloys is presented in Fig. 6. The cycle lives of the as-quenched (20 m/s) alloys prolonged significantly with increasing M content. When M content changed from 0 to 0.4, the cycle life of the  $M_x$  ( $M=Cu$ ) alloy increased from 86 to 99 cycles, for  $M_x$  ( $M=Al$ ) alloy from 86 to 134 cycles, and for  $M_x$  ( $M=Mn$ )

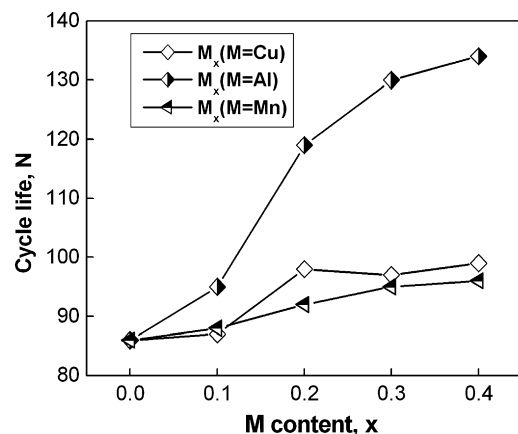


Fig. 6. M content dependence of the cycle life of the as-quenched (20 m/s) alloys.

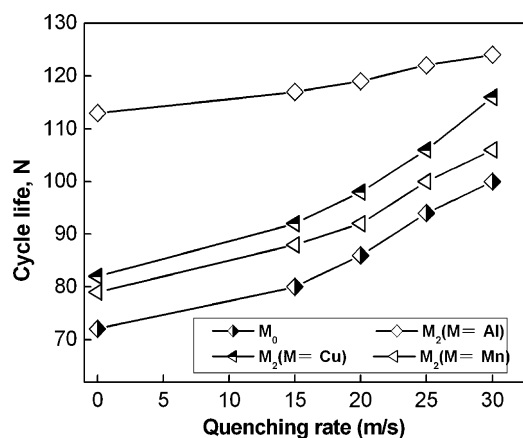


Fig. 7. The quenching rate dependence of the cycle life of  $M_0$  and  $M_2$  alloys.

alloy, from 86 to 96 cycles. The positive effect of three kinds of substitution elements on the cycle life of the alloys is in the sequence  $Al > Cu > Mn$ . The results shown in Fig. 7 indicated that the cycle life of the  $M_0$  and  $M_2$  ( $M = Cu, Al, Mn$ ) alloys prolonged with increasing the quenching rate. The fact that the substitution  $Cu, Al$  and  $Mn$  meliorates the cycle stability of the alloys probably is due to form a dense oxide film on the alloy surface, which can obviously intensify the anti-oxidation and anti-corrosion ability of the alloy electrode in alkaline electrolyte. A trace of amorphous phase can be found by SAD in the as-quenched  $Cu$  and  $Mn$  substituted alloys, which is helpful to meliorate the cycle stability of the alloy because an amorphous phase can increase not only the anti-pulverization ability but also the anti-corrosion capability of the alloy [8]. It is considered to be a perfect structure that amorphous film continuously distributes on the grain boundary of the electrode alloy, but the existed position of amorphous phase in the as-quenched experimental alloys needs to be further investigated. Two factors are responsible for rapid quenching extending the cycle life of the alloy. One of them is that the grain refinement by rapid quenching obviously augments the anti-pulverization capability of the alloy, and another is the formation of an amorphous phase by rapid quenching. The quenching rate is a decisive factor of the grain size and the amount of an amorphous phase for a fixed alloy, and the higher the quenching rate, the smaller the grain size and the larger the amount of amorphous phase. Therefore, it seems to be self-evident that the cycle life of the alloy increases with elevating the quenching rate.

#### 4. Conclusions

1. The substitution of  $M$  ( $M = Cu, Al$  and  $Mn$ ) for  $Ni$  engenders an inappreciable influence on the phase compositions of the as-cast and quenched  $La_{0.7}Mg_{0.3}Co_{0.45}Ni_{2.55-x}M_x$  ( $M = Cu, Al, Mn, x = 0, 0.1, 0.2, 0.3, 0.4$ ) alloys, but it increases the abundances of the  $LaNi_2$  phase in the as-cast alloys. The substitution of  $Cu$  and  $Mn$  is favourable to the formation of an amorphous phase, but  $Al$  substitution is unfavourable. The element substitution leads to enlarged of the lattice parameters and cell volumes of the alloys.
2. The substitution of  $Cu, Al$  and  $Mn$  decreased the capacity of the as-cast and quenched alloys, but it markedly improved their cycle stabilities. The negative function of element substitution on the capacity of the alloys is in the sequence  $Cu < Mn < Al$ , and its positive function on the cycle life of the alloys is in the sequence  $Al > Cu > Mn$ .
3. The rapid quenching notably impaired the discharge capacity and discharge voltage of the alloys, but it remarkably intensified the cycle stability of the alloys. The grain refinement and the formation of an amorphous phase resulted from the rapid quenching is responsible for rapid quenching enhancing the cyclic stability of alloy.

#### Acknowledgements

This work is supported by National Natural Science Foundation of China (50642033), Science and Technology Planned Project of Inner Mongolia, China (20050205) and Higher Education Science Research Project of Inner Mongolia, China (NJ05064).

#### References

- [1] T. Kohno, H. Yoshida, F. Kawashima, T. Inaba, I. Sakai, M. Yamamoto, M. Kanda, *J. Alloys Compd.* 11 (2003) L5–L7.
- [2] K. Kadir, T. Sakai, I. Uehara, *J. Alloys Compd.* 257 (1997) 115–121.
- [3] H.G. Pan, Y.F. Liu, M.X. Gao, Y.F. Zhu, Y.Q. Lei, Q.D. Wang, *J. Alloys Compd.* 351 (2003) 228–234.
- [4] A. Takasaki, K. Sasao, *J. Alloys Compd.* 404–406 (2005) 431–434.
- [5] J.J.G. Reilly, J.O. Besenhard (Eds.), *Metal Hydrides Electrodes, Handbook of Battery Materials*, Wiley, New York, 2000.
- [6] W.H. Lai, C.Z. Yu, *Chin. Battery* 26 (4) (1996) 189–191.
- [7] B. Liao, Y.Q. Lei, L.X. Chen, G.L. Lu, H.G. Pan, Q.D. Wang, *J. Alloys Compd.* 376 (2004) 186–195.
- [8] Y.H. Zhang, G.Q. Wang, X.P. Dong, S.H. Guo, J.M. Wu, X.L. Wang, *J. Alloys Compd.* 379 (2004) 298–304.